Exploring Massive Neutron Stars Towards the Mass Gap: Constraining the High Density Nuclear Equation of State¹

Zenia Zuraiq^{a,*}, Banibrata Mukhopadhyay^a, and Fridolin Weber^{b,c}

^a Department of Physics, Indian Institute of Science, Bangalore, 560012 India

^b Department of Physics, San Diego State University, San Diego, CA 92182 USA

^c Center for Astrophysics and Space Sciences, University of California at San Diego, La Jolla, CA 92093 USA * e-mail: zeniazuraig@iisc.ac.in

Received September 30, 2023; revised November 21, 2023; accepted November 21, 2023

Abstract—Due to the high-density nuclear matter equation of state (EOS) being as yet unknown, neutron stars (NSs) do not have a confirmed limiting "Chandrasekhar" type maximum mass. However, observations of NSs (PSR J1614-2230, PSR J0348+0432, PSR J0740+6620, PSR J0952-0607) indicate that the NS's limiting mass, if there is any, could be well over $2M_{\odot}$. On the other hand, there seems to be an observational mass gap (of around $2.5-5M_{\odot}$) between the lightest black hole and the heaviest NS. Therefore, the "massive NSs" are prime candidates to fill that gap. Several NS EOSs have been proposed using both microscopic and phenomenological approaches. In this project, we look at a class of phenomenological nuclear matter EOSs—relativistic mean field models—and see what kind of NS is formed from them. We compute the maximum mass supported by each model EOS to observe if the mass of the NS is indeed in the "massive" NS (>2 M_{\odot}) regime. We also observe the effects of including exotic particles (hyperons, Δs) in the NS EOS and how that affects the NS mass. However, only by introducing the magnetic field, i.e. for magnetized anisotropic NSs, we find the mass exceeding $2.5M_{\odot}$. Using tidal deformability constraints from gravitational wave observations, we place a further check on how physical the EOS and NSs are.

Keywords: nuclear matter in neutron stars, general relativity, gravitational waves, nuclear astrophysics, nuclear matter, neutron stars and pulsars, astrophysical electromagnetic fields

DOI: 10.1134/S1063772923140214

1. INTRODUCTION

Even after half a century since the original discovery of the first pulsar [1], the precise constituents of neutron stars (NSs) and their radius are still not well constrained. This also leads to the fact that NSs do not have a well-defined mass-limit, unlike the Chandrasekhar mass-limit of white dwarfs. Nevertheless, attempts have been made to establish the NS masslimit (e.g. [2]), which are however insensitive to the equation of state (EOS). On the other hand, it is wellknown that above nuclear saturation density, EOSs are highly uncertain due to the uncertainity of the strong interaction coupling constant. This leads to the varieties of possible mass-radius relations and mass-limits. Additional uncertainty arises when a NS is (highly) magnetized, due to the uncertainty of the magnetic field geometry and the central (or maximum) magnetic field of the star. This has been indeed shown to be the case for NSs and white dwarfs [3, 4].

It is believed that the lightest mass of an astrophysical black hole could be as low as $3.3M_{\odot}$ [5] (but also see [6]) and the heaviest NS is $2.35M_{\odot}$ [7]. Hence, there seems to be a mass gap. On the other hand, the recent gravitational wave observation GW190814 argues for the existence of a compact object of mass $2.5-2.67M_{\odot}$, in the mass gap. While it could be a primordial black hole, there is no observational evidence for such objects yet. Further, an astrophysical black hole seems implausible to have such a tiny mass [8]. Can this be a NS? Conventional NS EOSs do not seem to suggest their mass as high as $2.5M_{\odot}$, particularly when hyperons are assumed to emerge at higher density. Can other physics help to increase the stellar mass?

Here, we show that (moderately) strong magnetic fields with central field $\lesssim 10^{18}$ G, along with a stiffer EOS, can lead to NSs well belonging to the mass gap.

Paper presented at the Fifth Zeldovich meeting, an international conference in honor of Ya.B. Zeldovich held in Yerevan, Armenia on June 12–16, 2023. Published by the recommendation of the special editors: R. Ruffini, N. Sahakyan and G.V. Vereshchagin.

We further report that the results also depend on the geometry and profile of the magnetic field. They are also in accordance with the tidal deformability limit.

2. FORMALISM

We describe magnetized, anisotropic, spherically symmetric NSs by modified Tolman—Oppenheimer—Volkoff (TOV) equations [3], given by

$$\frac{dm}{dr} = 4\pi r^{2} \left(\rho + \frac{B^{2}}{8\pi} \right),$$

$$\frac{-(\rho + p_{r}) \frac{\left(4\pi r^{3} \left(p_{r} - \frac{B^{2}}{8\pi} \right) + m \right)}{r(r - 2m)} + \frac{2}{r} \Delta}{\left(1 - \frac{d}{d\rho} \left(\frac{B^{2}}{8\pi} \right) \left(\frac{d\rho}{dp_{r}} \right) \right)}$$
(1)
$$\frac{-\left(\rho + p_{r} + \frac{B^{2}}{4\pi} \right) \frac{\left(4\pi r^{3} \left(p_{r} + \frac{B^{2}}{8\pi} \right) + m \right)}{r(r - 2m)} + \frac{2}{r} \Delta}{\left(1 + \frac{d}{d\rho} \left(\frac{B^{2}}{8\pi} \right) \left(\frac{d\rho}{dp_{r}} \right) \right)}$$
(for TO),

where the symbols have their usual meanings. The effective anisotropy of the system $\Delta = (p_t - p_r + B^2/4\pi)$ for radially oriented (RO) fields, and $\Delta = (p_t - p_r - B^2/8\pi)$ for transversely oriented (TO) fields.

To close the system of equations, we introduce a model functional form for Δ based on the general parametric form, first introduced by Bowers and Liang [9], and further modified to include the effects of magnetic field by our group [3], given by

$$\Delta = \kappa r^2 \frac{(\rho + p_r) \left(\rho + 3p_r - \frac{B^2}{4\pi}\right)}{1 - \frac{2m}{r}} \quad \text{(for RO)},$$

$$\Delta = \kappa r^2 \frac{\left(\rho + p_r + \frac{B^2}{4\pi}\right) \left(\rho + 3p_r + \frac{B^2}{2\pi}\right)}{1 - \frac{2m}{r}} \quad \text{(for TO)}.$$

Following previous work [10], we restrict κ values to the range [-2/3,2/3]. We further need to supplement with the equation of state (EOS) and magnetic field profile to solve the set of equations.

2.1. Magnetic Field Profile

We introduce a density-dependent magnetic field in the star [11, 12], given by

$$B(\rho) = B_s + B_0 \left[1 - \exp \left\{ -\eta \left(\frac{\rho}{\rho_0} \right)^{\gamma} \right\} \right], \quad (3)$$

which describes the magnitude of the field at a given density (hence the radius of the star). Here, B_s corresponds to the surface field of the star, B_0 controls the field at the center, and η and γ are model parameters that control how the field decays from center to surface. Throughout this work, we have chosen B_s to be 10^{13} G. The results are mostly independent of B_s as increasing the surface field to 10^{15} G does not have a practical effect on the results.

2.2. Equations of State

We consider a selection of phenomenological EOSs, constructed under the relativistic mean field (RMF) approximation. Matter is modeled at the hadron level (quantum hadrodynamics). The baryon-baryon interactions present in NS matter are modeled in terms of meson fields as mediators. The meson field strengths are then set to their mean values as per the RMF approximation. We have included three such meson fields — the scalar meson $\sigma,$ which describes attraction between baryons; the vector meson $\omega,$ which describes repulsion; and the isovector meson $\rho,$ which is required to explain isospin asymmetric interactions.

EOSs are constrained in two ways—by NS observations, and by the properties of nuclear matter at saturation density. We choose a few EOSs—GM1L [13], SWL [14], DD2 [15], DD-ME1 [16], and DD-ME2 [17]—that best satisfy both the above constraints.

At their cores. NSs can have densities several times to order(s) of magnitude higher than the nuclear saturation density. As a result, the presence of exotic particles is energetically favorable in such conditions. "Exotic" particles are those that do not exist in stable form under terrestrial conditions. Along with pure nucleonic (npeu) EOSs, we have also considered hyperon and Δ admixed (npeu – $Y\Delta$) EOSs. The inclusion of hyperonic matter has been done by including meson-hyperon couplings based on the SU(3) ESC08 model, and the inclusion of Δ particles done by including a near-universal meson- Δ coupling, with $x_{i\Delta} = g_{i\Delta}/g_{iN} = 1.2$, where g represents the coupling constants; the subscript Δ indicates the Δ particles, N the nucleons, and i represents the mesons mentioned above.

Figure 1 shows that the pure nucleonic EOSs are much stiffer. This aligns with the hyperon softening/hyperon puzzle explored in past literature. Includ-

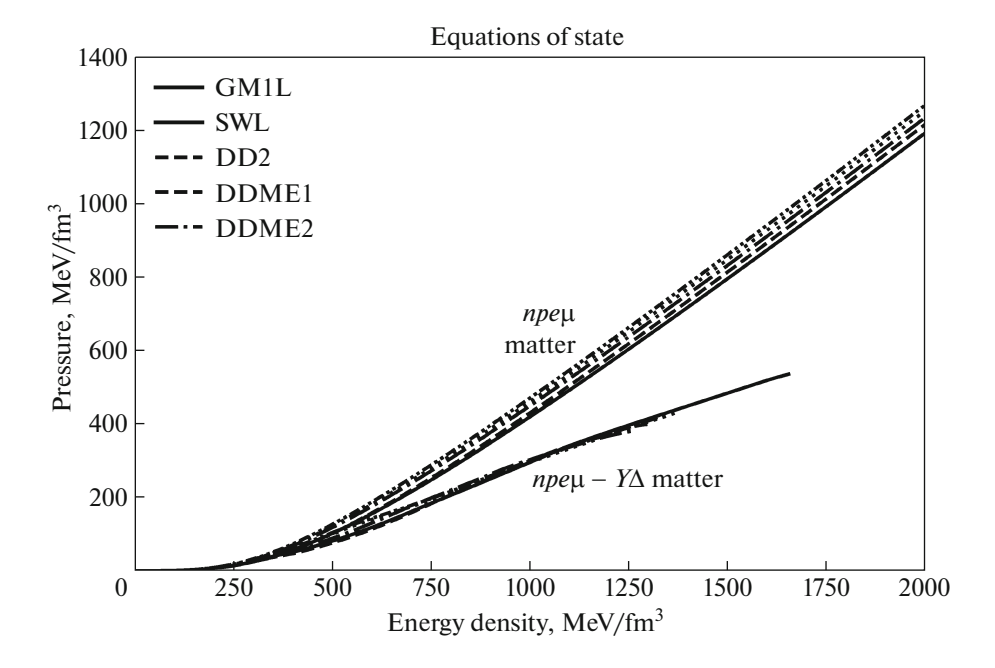


Fig. 1. EOSs for $npe\mu$ matter (upper branch) and hyperon- Δ admixed cases (lower branch).

ing additional baryonic degrees of freedom in the form of the exotic particles, in this case, hyperons and Δs , soften the EOS by minimizing the total energy.

2.3. Tidal Deformability

An additional constraint on the NS EOS is the tidal deformability parameter. In the presence of an external gravitational field (ϵ_{ij}) , a star develops a quadrupole moment (Q_{ij}) such that $Q_{ij} = -\lambda \epsilon_{ij}$, where λ is the tidal deformability of the star.

Theoretically, one can link λ to the dimensionless second Love number k_2 , arising from gravitational multipole expansion, as $\lambda = (2/3)k_2R^5$ [18]. If λ is recast into a dimensionless form, we obtain $\Lambda = \lambda/M^5 = (2/3)k_2C^{-5}$, where C = M/R is the compactness of the star.

To compute k_2 , we solve the following differential equation for H(r), given by,

$$H'' + H' \left[\frac{2}{r} + e^{\lambda} \left(\frac{2m(r)}{r^2} + 4\pi r (p_r - \rho) \right) \right]$$

$$+ H \left[4\pi e^{\lambda} \left(4\rho + 8p_r + \frac{\rho + p_r}{Ac_s^2} (1 + c_s^2) \right) - \frac{6e^{\lambda}}{r^2} - v'^2 \right] = 0.$$
(4)

Here, H(r) is a radial function arising from the static, linearized perturbations of the Einstein equations. As we are solving for k_2 , we restrict ourselves to the l=2, static, even-parity perturbations of the perturbation metric. The other quantities are $A=dp_t/dp_r$, $c_s^2=dp_r/d\rho$ (the speed of sound squared), $e^{\lambda}=\left[1-2m/r\right]^{-1}$, and $\nu'=(2e^{\lambda}(m+4\pi p_r r^3)/r^2$. For isotropic stars, A=1.

On obtaining H(r) by solving Eq. (4) simultaneously with our system of equations, one can compute the tidal love number k_2 as

$$k_{2} = (8/5)C^{5}(1 - 2C^{2})[2 - y_{R} + 2C(y_{R} - 1)]$$

$$\times \{2C(6 - 3y_{R} + 3C(5y_{R} - 8)) + 4C^{3}[13 - 11y_{R} + C(3y_{R} - 2) + 2C^{2}(1 + y_{R})] + 3(1 - 2C)^{2}$$

$$\times [2 - y_{R} + 2C(y_{R} - 1)]\log(1 - 2C)\}^{-1},$$
(5)

where, $y_R = rH'(R)/H(R)$, with R being the radius of the star.

In recent years, due to gravitational wave observations, observational constraints have been placed on the dimensionless tidal deformability parameter. From the binary NS merger event GW170817, the dimensionless tidal deformability at $1.4 M_{\odot}$ has been constrained to be $\Lambda_{1.4} < 800$ [20] and $\Lambda_{1.4} < 580$ [21]. The difference between these limits is parameter dependent, and we have enforced both in our subsequent analysis.

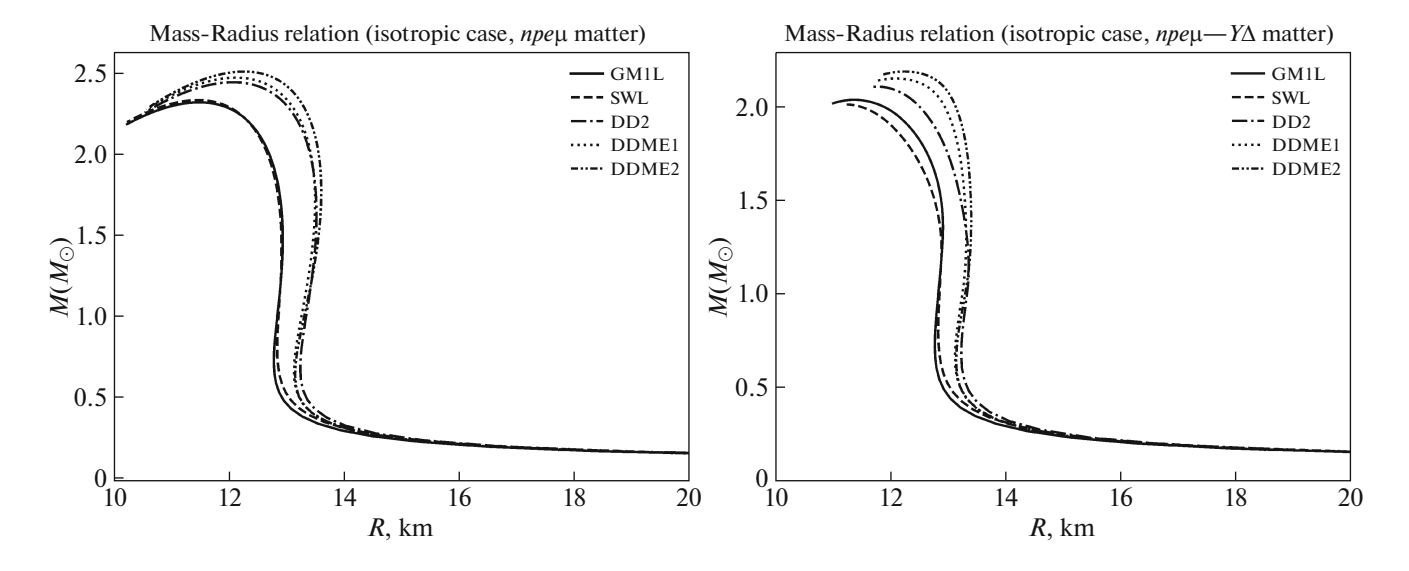


Fig. 2. Mass-radius curves for isotropic NSs constructed from $npe\mu$ matter (left) and hyperon- Δ admixed EOSs (right).

3. RESULTS AND DISCUSSIONS

We study magnetized NSs constructed from different RMF EOSs. We solve Eqs. (1)—(3), supplemented by EOS, for a series of central densities. Each EOS input generates a family of stars, parameterized by the central density.

The zero anisotropy and nonmagnetic field case results in completely isotropic NSs, showing pure EOS effects. As seen from Fig. 1, $npe\mu - Y\Delta$ EOSs are much softer, and we expect them to support less mass as compared to the pure nucleonic $npe\mu$ EOS. This is indeed found in the mass-radius relation shown by Fig. 2, when $npe\mu$ EOSs support NS of masses as high as $2.51\,M_\odot$, whereas $npe\mu - Y\Delta$ EOSs support masses upto $2.18\,M_\odot$ (Table 1).

As the presence of exotic particles is well favored energetically, we continue the rest of the analysis using the $npe\mu - Y\Delta$ EOSs. Moreover, the tidal deformabil-

Table 1. Numerical values for the physical parameters of isotropic NSs, both by inclusion of exotic particles, and for pure nucleonic matter

EOS	Pure nue		Incl. hyperons and Δs $(npe\mu - Y\Delta)$		
	$M_{\rm max}~(M_{\odot})$	R (km)	$M_{\rm max}~(M_{\odot})$	R (km)	
GM1L	2.3235	11.45	2.0348	11.365	
SWL	2.3371	11.43	2.0098	11.246	
DD2	2.4474	11.94	2.1049	11.786	
DDME1	2.4703	12.123	2.1486	12.096	
DDME2	2.5077	12.242	2.1857	12.248	

ity analysis (Fig. 3) shows us that all the $npe\mu - Y\Delta$ EOSs come under atleast one of the observational bounds for $\Lambda_{1.4}$, whereas the same is not true for the purely nucleonic counterparts.

Therefore, through pure $npe\mu - Y\Delta$ EOS effects, one can explain NS of masses $>2M_{\odot}$, but not the mass gap range objects (masses $>2.5M_{\odot}$). This motivates us to turn to the additional physics of magnetic fields and/or anisotropy.

We fix our anisotropy parameter, κ , to be 0.5 throughout our subsequent analysis. We start with a magnetic field profile defined by $\eta = 0.2$, $\gamma = 2$ and choose B_0 as 0.9×10^{18} G and 1.2×10^{18} G for TO, and 0.6×10^{18} G and 0.9×10^{18} G for RO fields. Throughout this work we choose B_0 such that the maximum field is below 3×10^{18} G. As shown earlier [22], above this value, the microscopic effects of field on the EOS, i.e., Landau quantization, become important, which is not included in our formalism. The general shape of the magnetic field profile, and the resulting mass-radius curves and tidal deformability, for the DDME2 EOS, are shown in Fig. 4. The limiting mass and corresponding radius are given in Table 2.

We see that similar to the earlier results [3], even at zero field, due to the presence of anisotropy parameter κ , the mass is enhanced from the isotropic case. Further adding the magnetic field to this anisotropic star can increase or decrease the mass based on the field orientation. This trend is observed across all the EOSs studied. Larger TO fields further increase the mass, whereas larger RO fields tend to decrease the mass.

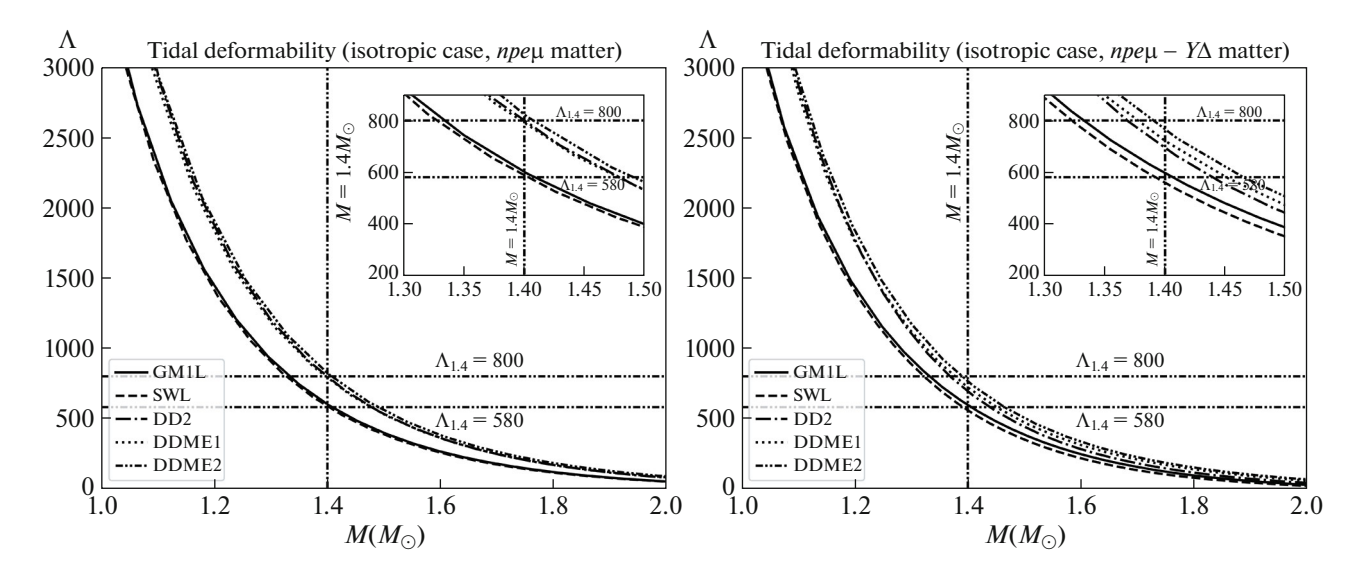


Fig. 3. Tidal deformability for isotropic NSs constructed from $npe\mu$ matter (left) and hyperon- Δ admixed EOSs (right).

For the DDME2 EOS, at $B_0 = 1.2 \times 10^{18}$ G, we obtain limiting mass as high as $2.76M_{\odot}$.

On computing the tidal deformability of these cases (Fig. 4), we find that extremely high fields appear to be ruled out. Particularly, $B_0 = 1.2 \times 10^{18}$ G fails to meet either of the observational bounds on $\Lambda_{1.4}$. However, it is important to note that this result is dependent on the magnetic field profile (the particular choice of η and γ).

To check if we are able to salvage high fields in our NS while meeting the tidal deformability constraint, we next look at an alternate magnetic field profile with $\eta = 0.01$ and $\gamma = 2$. The shape of this profile and the results are shown in Fig. 5. For this profile, we consider TO fields with four appropriate B_0 such that $B_{\text{max}} = 0.14 \times 10^{18} \,\text{G}$, $B_{\text{max}} = 0.28 \times 10^{18} \,\text{G}$, $B_{\text{max}} = 0.79 \times 10^{18} \,\text{G}$, and $B_{\text{max}} = 1.32 \times 10^{18} \,\text{G}$. As this profile exhibits a faster decay of the field within the star, it results in a lowered magnetic pressure gradient

(Lorentz force). This ultimately leads to masses lower than those of the previous profile considered above. Table 2 shows that the magnetic field adds significant mass to the star only at $\approx 0.5 \times 10^{18}$ G above.

On the stability ground (by magnetic to gravitational energy ratio: $E_{\rm mag}/E_{\rm grav}$), we find that this profile leads to much more stable stars, even at high fields. Further, on computing the tidal deformability, all the magnetized stars, including the high $B_{\rm max}$ case, satisfy even the stricter limit: $\Lambda_{1.4} < 580$, as seen in Fig. 5.

This indicates that all our results, starting from the limiting mass to the tidal deformability, are not only dependent on the magnitude of the (central/maximum) magnetic fields, but also the field profile within the star. Highly magnetized NSs, possibly serving as mass gap candidates, can exist while satisfying tidal deformability and stability constraints, with the right choice of profile.

Table 2. Numerical values for the physical parameters of magnetized, anisotropic ($\kappa = 0.5$) NSs from the DDME2 EOS

Field profile: $\eta = 0.2$, $\gamma = 2$				Field profile: $\eta = 0.01$, $\gamma = 2$			
$B_{\text{max}} (10^{18} \text{ G})$	$M_{ m max}~(M_{\odot})$	R (km)	$E_{ m mag}/E_{ m grav}$	$B_{\text{max}} (10^{18} \text{ G})$	$M_{ m max}~(M_{\odot})$	R (km)	$E_{ m mag}/E_{ m grav}$
0.899 (RO)	2.2641	11.695	0.127	0	2.5400	12.924	_
0.599 (RO)	2.4128	12.408	0.057	0.14 (TO)	2.5409	12.922	0.0006
0	2.540	12.924	_	0.28 (TO)	2.5434	12.921	0.0026
0.895 (TO)	2.6706	13.436	0.118	0.79 (TO)	2.5696	12.898	0.024
1.188 (TO)	2.7645	13.752	0.196	1.32 (TO)	2.6158	12.875	0.064

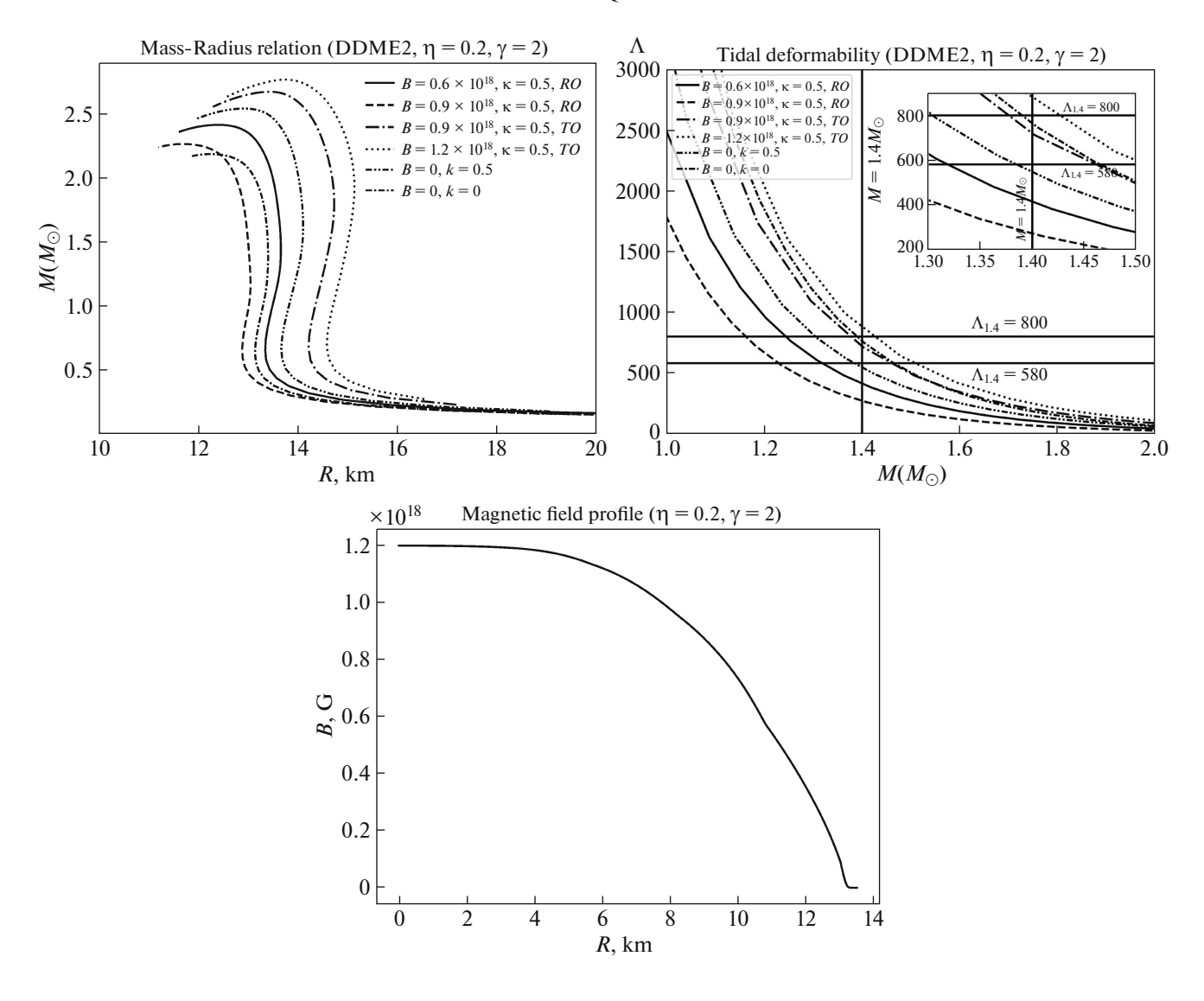


Fig. 4. Mass-radius relation (top left) and tidal deformability (top right) for magnetized ($\eta = 0.2$, $\gamma = 2$), anisotropic ($\kappa = 0.5$) NSs constructed from DDME2 EOS. Representative field profile within a given star given at the bottom.

4. CONCLUSIONS

Precise radius measurement of NSs is still a challenge and the underlying radius range is still not well-founded. However, combined NICER and gravitational wave data have started constraining the radius with a range of 11-13 km for a $1.4M_{\odot}$ NS. This also helps to sort out realistic EOSs. Nevertheless, still, there are lots of other uncertainties, including the questions of maximum mass and magnetic fields in stable NSs. In this paper, we have explored a variety of $npe\mu - Y\Delta$ EOSs, particularly stiffer ones, i.e. with the possible emergence of hyperons at high density, yet found the maximum mass of a NS to be $2.18M_{\odot}$. This is still well below the mass gap. By introducing anisotropic effects of matter at high density, the mass could be increased to $2.54M_{\odot}$. However, we have found that

to construct a NS well within the mass gap, the magnetic field is indispensable. For example, a toroidally dominated magnetized anisotropic (due to matter and magnetic effects) NS with a central field $\sim 10^{18}$ G could even be $2.7M_{\odot}$.

However, we have further checked the constraints from stability and tidal deformability. Thence, we have obtained the maximum mass to be about $2.6M_{\odot}$. This argues that the lighter component of GW190814 could be a NS filling in the mass gap. With more observations, particularly in gravitational wave astronomy, we expect to see more such mass gap objects, some of which could be massive, magnetized NSs. All the above inferences, however, are based on one particular magnetic field profile and two sets of parameters. Moreover, a specific model of anisotropy is assumed

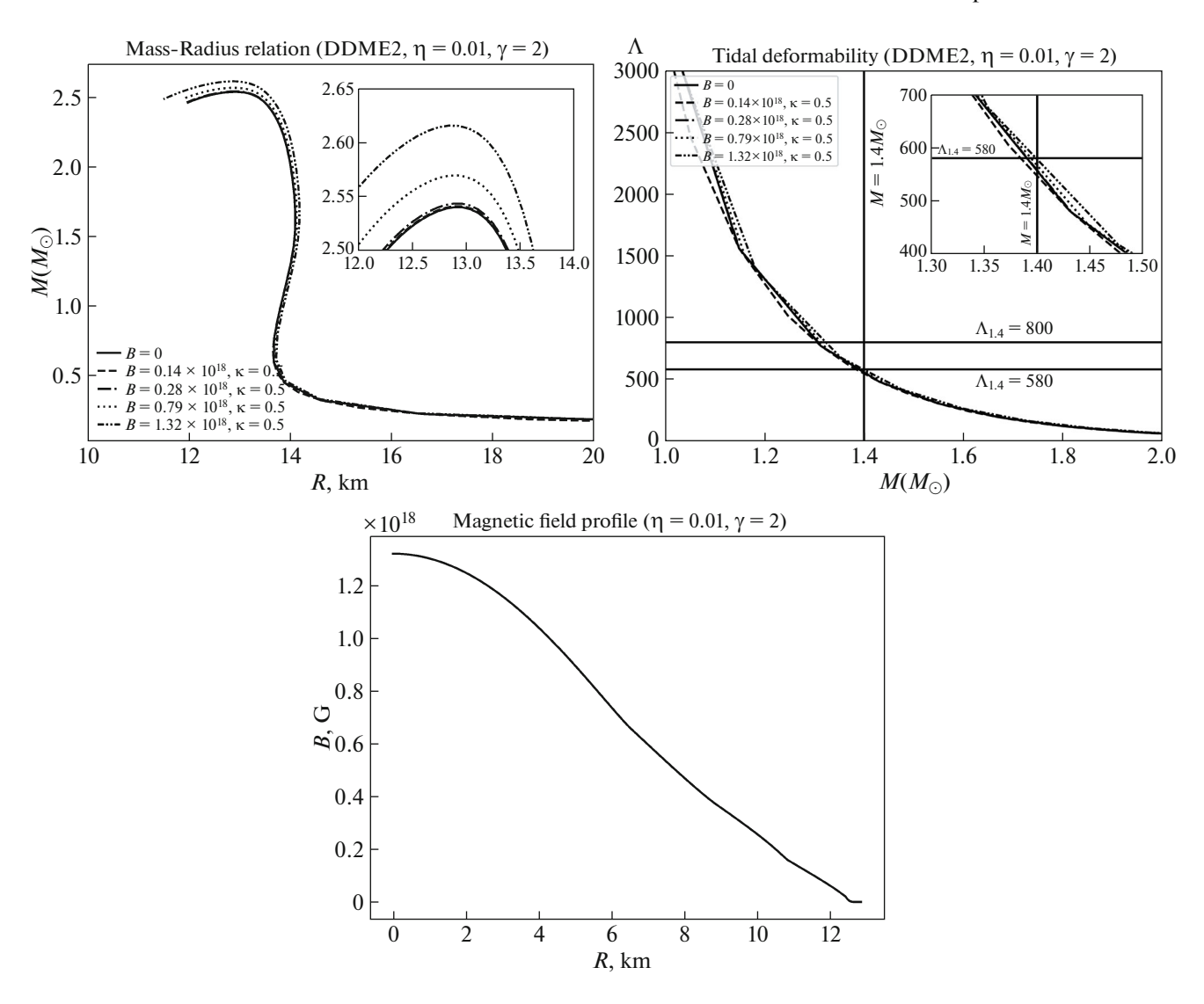


Fig. 5. Mass-radius relation (top left) and tidal deformability (top right) for magnetized ($\eta = 0.01, \gamma = 2$), anisotropic ($\kappa = 0.5$) NSs constructed from DDME2 EOS. Representative field profile within a given star given at the bottom.

for the present purpose. To establish the results firmly, other field profiles and model anisotropy should be explored. Nevertheless, our findings suggest that massive NSs belonging to the mass gap should have internal fields as high as 10¹⁸ G.

ACKNOWLEDGMENTS

ZZ and BM acknowledge Debabrata Deb of IMSc for discussion about the tidal deformability, and Somnath Mukhopadhyay of NIT-Trichy for comments.

FUNDING

ZZ acknowledges the Prime Minister's Research Fellows (PMRF) scheme, with Ref. no. TF/PMRF-22-7307, for providing fellowship. BM thanks SERB, India, with

Ref. no. CRG/2022/003460, for partial support towards this research. FW acknowledges financial support provided by the U.S. National Science Foundation under Grant no. PHY-2012152.

CONFLICT OF INTEREST

The authors of this work declare that they have no conflicts of interest.

REFERENCES

- A. Hewish, S. J. Bell, J. D. H. Pilkington, P. F. Scott, and R. A. Collins, Nature (London, U.K.) 217, 709 (1967).
- C. E. Rhoades and R. Ruffini, Phys. Rev. Lett. 32, 324 (1974).

- 3. D. Deb, B. Mukhopadhyay, and F. Weber, Astrophys. J. **922**, 149 (2021).
- D. Deb, B. Mukhopadhyay, and F. Weber, Astrophys. J. 926, 66 (2022).
- T. A. Thompson et al., Science (Washington, DC, U. S.) 366, 637 (2019).
- P. J. van den Heuvel and Th. M. Tauris, Science (Washington, DC, U. S.) 368, eaba3282 (2020).
- 7. R. W. Romani, D. Kandel, A. V. Filippenko, T. G. Brink, and W. Zheng, Astrophys. J. **934**, L17 (2022).
- A. I. MacFadyen and S. E. Woosley, Astrophys. J. 524, 262 (1999).
- R. L. Bowers and E. P. T. Liang, Astrophys. J. 188, 657 (1974).
- H. O. Silva, C. F. B. Macedo, E. Berti, and L. C. B. Crispino, Class. Quantum Grav. 32, 145008 (2015).
- 11. D. Bandhopadhyay, S. Chakrabarty, and S. Pal, Phys. Rev. Lett. **79**, 2176 (1997).
- 12. D. Bandhopadhyay, S. Pal, and S. Chakrabarty, J. Phys. G: Nucl. Part. Phys. 24, 1647 (1998).

- 13. N. K. Glendenning and S. A. Moszkowski, Phys. Rev. Lett. **67**, 2414 (1991).
- 14. W. M. Spinella, Ph. D. Thesis (Claremont Graduate Univ., San Diego State Univ., 2017).
- 15. S. Typel, G. Röpke, T. Klähn, D. Blaschke, and H. H. Wolter, Phys. Rev. C **81**, 015803 (2010).
- T. Nikšić, D. Vretenar, P. Finelli, and P. Ring, Phys. Rev. C 66, 024306 (2002).
- G. A. Lalazissis, T. Nikšić, D. Vretenar, and P. Ring, Phys. Rev. C 71, 024312 (2005).
- 18. T. Hinderer, Astrophys. J. 677, 1216 (2008).
- 19. B. Biswas and S. Bose, Phys. Rev. D 99, 104002 (2019).
- 20. B. P. Abbott et al., Phys. Rev. Lett. 119, 161101 (2017).
- 21. B. P. Abbott et al., Phys. Rev. Lett. 121, 161101 (2018).
- M. Sinha, B. Mukhopadhyay, and A. Sedrakian, Nucl. Phys. A 898, 43 (2013).

Publisher's Note. Pleiades Publishing remains neutral with regard to jurisdictional claims in published maps and institutional affiliations.